

Role of the PH domain in regulating in vitro autophosphorylation events required for reconstitution of PDK1 catalytic activity

Xinxin Gao, Thomas K. Harris *

*Department of Biochemistry and Molecular Biology, University of Miami,
Miller School of Medicine, P.O. Box 016129, Miami, FL 33101-6129, USA*

Received 6 May 2006

Available online 15 June 2006

Abstract

In addition to its catalytic domain, phosphoinositide-dependent protein kinase-1 (PDK1) contains a C-terminal pleckstrin homology (PH) domain, which binds the membrane-bound phosphatidylinositol (3,4,5)-triphosphate [PI(3,4,5)P₃] second messenger. Here, we report in vitro kinetic, phosphopeptide mapping, and oligomerization studies that address the role of the PH domain in regulating specific autophosphorylation events, which are required for PDK1 catalytic activation. First, ‘inactive’ unphosphorylated forms of N-terminal His₆ tagged full length (His₆-PDK1) and catalytic domain constructs [His₆-PDK1(ΔPH)] were generated by treatment with Lambda protein phosphatase (λPP). Reconstitution of λPP-treated His₆-PDK1(ΔPH) catalytic activity required activation loop Ser-241 phosphorylation, which occurred only upon *trans*-addition of ‘active’ PDK1 with an apparent bimolecular rate constant of $^{app}k_{1S241} = 374 \pm 29 \text{ M}^{-1} \text{ s}^{-1}$. In contrast, full length λPP-treated His₆-PDK1 catalyzed Ser-241 *cis*-autophosphorylation with an apparent first-order rate constant of $^{app}k_{1S241} = (5.0 \pm 1.5) \times 10^{-4} \text{ s}^{-1}$ but remained ‘inactive’. Reconstitution of λPP-treated His₆-PDK1 catalytic activity occurred only when autophosphorylated in the presence of PI(3,4,5)P₃ containing vesicles. PI(3,4,5)P₃ binding to the PH domain activated apparent first-order Ser-241 autophosphorylation by 20-fold [$^{app}k_{1S241} = (1.1 \pm 0.1) \times 10^{-2} \text{ s}^{-1}$] and also promoted biphasic Thr-513 *trans*-autophosphorylation [$^{app}k_{2T513} = (4.9 \pm 1.1) \times 10^2 \text{ M}^{-1} \text{ s}^{-1}$ and $^{app}k_{3T513} = (1.5 \pm 0.2) \times 10^3 \text{ M}^{-1} \text{ s}^{-1}$]. The results of mutagenesis studies suggest that Thr-513 phosphoryla-

* Corresponding author. Fax: +1 305 243 3955.

E-mail address: tkharris@miami.edu (T.K. Harris).

tion may cause dissociation of autoinhibitory contacts formed between the contiguous regulatory PH and catalytic kinase domains.

© 2006 Elsevier Inc. All rights reserved.

Keywords: Phosphoinositide-dependent protein kinase-1; Phosphoinositide signaling; Protein kinase; Autoinhibition; Autophosphorylation; Oligomerization; Phosphopeptide mapping; Sedimentation equilibrium; Agc kinases

1. Introduction

Phosphoinositide-dependent protein kinase-1 (PDK1)¹ is a member of the AGC sub-family of serine–threonine protein kinases [1]. Among these kinases, amino acid sequences are conserved in a segment of the kinase domain known as the activation loop or T-loop, as well as in a segment C-terminal to the kinase domain known as the hydrophobic motif; and phosphorylation sites or acidic residues in these regions play important roles in their catalytic regulation and/or stability. In contrast to other AGC kinases, PDK1 does not possess a hydrophobic motif C-terminal to its catalytic domain. Rather, a pleckstrin homology (PH) domain resides at the C-terminus, which has been shown to be required for phosphatidylinositol 3-kinase (PI3K)-dependent co-localization and *trans*-phosphorylation of protein kinase B (PKB/Akt) [2–8]. Although much progress has been achieved towards describing the diverse array of downstream protein kinase targets activated by PDK1 [9,10], considerable questions remain regarding the mechanism by which PDK1 catalytic activation is regulated.

Cellular localization studies of green fluorescent protein (GFP)-tagged full length PDK1 [11] confirmed previous studies [12] that PDK1 is mainly cytosolic, with a small fraction at the membrane, and is excluded from the nucleus in unstimulated HEK 293 cells; and localization of PDK1 is not affected by either agonists or inhibitors of PI3K. Furthermore, the high basal activity of PDK1 equally observed in both unstimulated and PI3K-activated cells supports the notion that PDK1 is constitutively active and that its activity is not critically regulated [13]. Like other members of the AGC kinase family, PDK1 requires phosphorylation of Ser-241 of its activation loop for catalytic activity, and both *in vivo* and *in vitro* evidence suggest that PDK1 catalyzes autophosphorylation of this site [13–17]. Also, it has been shown that *in vivo* co-expression of PDK1 with v-Src leads to tyrosine phosphorylation (Tyr-9 and Tyr-373/376), which further enhances PDK1 catalytic activity [14].

¹ *Abbreviations used:* AMPPNP, β,γ -imidoadenosine 5'-triphosphate; ATP, adenosine 5'-triphosphate; 2,5-DHB, 2,5-dihydroxybenzoic acid; GSK3, glycogen synthase kinase-3; His₆-PDK1, N-terminal His₆ affinity tagged recombinant 'full length' PDK1 (residues 51–556); His₆-PDK1(Δ PH), N-terminal His₆ affinity tagged recombinant catalytic domain of PDK1 (residues 51–359); HM, hydrophobic motif; I(1,3,4,5)P₄, D-myo-inositol (1,3,4,5)-tetrakisphosphate; I(1,3,4,6)P₄, D-myo-inositol (1,3,4,6)-tetrakisphosphate; I(1,3,4,5)P₄, D-myo-inositol (1,4,5)-triphosphate; λ PP, Lambda protein phosphatase; MEKK1, MEK kinase-1; MSK, mitogen- and stress-activated protein kinase; PC, 1,2-dioleoyl-*sn*-glycerol-3-phosphocholine; PDK1, phosphoinositide-dependent protein kinase-1; PH, pleckstrin homology; PHLPP, PH domain leucine-rich repeat protein phosphatase; PIF, PDK1-interacting fragment; PI3K, phosphatidylinositol 3-kinase; PI(3,4)P₂, *sn*-1-stearoyl-2-arachidonoyl D-phosphatidylinositol (3,4)-diphosphate; PI(3,4,5)P₃, *sn*-1-stearoyl-2-arachidonoyl D-phosphatidylinositol (3,4,5)-triphosphate; PKA, cAMP-dependent protein kinase; PKB, protein kinase B; PKC, Ca²⁺-activated protein kinase; PKG, protein kinase G; PKN, protein kinase N; PS, 1,2-dioleoyl-*sn*-glycerol-3-phosphol-serine; RSK, 90 kDa 40 S ribosomal protein S6 kinase; SGK, serum- and glucocorticoid-induced protein kinase; S6K, 70 kDa 40 S ribosomal protein S6 kinase.

In addition to Ser-241, Tyr-9, and Tyr-373/376, PDK1 has also been shown to be significantly phosphorylated in vivo at Ser-25 [13,14], Ser-393 [13], and Ser-396 [13,15,16]. But, upstream kinases for phosphorylation of these sites have yet to be identified. Other sites of autophosphorylation include Thr-33 [14], Ser-410 [13,14], and Thr-513 [14–17]. While no significant effect on PDK1 catalytic activity occurred upon Ser/Ala mutations of either Ser-25, Ser-410, Ser-393, or Ser-396 [13], mutating Thr-516 of mouse PDK1 to glutamate (homologous to Thr-513 in human PDK1) caused constitutive activation of mPDK1 towards phosphorylation of PKB in cells [15]. This is particularly interesting since Thr-513 is located in the C-terminal PH domain, as the results of other in vivo studies suggested a role of the PH domain in modulating PDK1-catalyzed phosphorylation of PKB [18,19].

X-ray structural studies indicated that the C-terminal PH domain of PDK1 (residues 408–556) possesses several unique features not previously observed in other PH domains [11]. First, the PDK1 PH domain contains an additional hydrophobic core or ‘bud’ located at the N-terminus region that joins to the PDK1 catalytic kinase domain. This ‘bud’ consists of two additional β strands followed by a long α helix, and it has not been observed in any other crystallized PH domain. While the functional role of the ‘bud’ region remains enigmatic, the additional observation that the PDK1 PH domain phosphoinositide binding pocket is significantly more spacious than other phosphoinositide binding PH domains explained the ability of PDK1 to efficiently bind numerous phosphoinositides [e.g., PI(3,4,5)P₃, PI(3,4)P₂, PI(4,5)P₂, PI(3,5)P₂, and PI(3)P] and inositol polyphosphates [e.g., I(1,3,4,5)P₄, I(1,3,4,6)P₄, I(1,3,4,5,6)P₅, I(3,4,5,6)P₄, IP₆, and SPP-IP₅] [5,11,12].

Previously, we described optimized conditions for baculovirus-mediated expression of His₆-PDK1 in Sf9 insect cells [20]. A homogeneous preparation of unphosphorylated His₆-PDK1 was further generated by treatment with Lambda protein phosphatase (λ PP). The Sf9-purified and λ PP-treated forms of His₆-PDK1 were characterized by isoelectric focusing (IEF) gel electrophoresis, Western analyses with specific phosphospecific antibodies, and steady-state kinetic analyses with the model peptide substrate PDK1-Tide. λ PP-treated His₆-PDK1 showed an \sim 80-fold decreased $V_{\max} = 2.4 \pm 0.4$ nmol/min/mg and \sim 4-fold increased $K_m = 217 \pm 61$ μ M compared to Sf9-purified His₆-PDK1.

In this paper, we report the results of mechanistic studies that address the role of the PH domain in regulating specific in vitro autophosphorylation events, which are required for reconstitution of catalytic activity in λ PP-treated His₆-PDK1. The results of these studies provide evidence in support that (i) the PH domain activates Ser-241 *cis*-autophosphorylation, (ii) the PH domain autoinhibits kinase catalytic activation of Ser-241 mono-phosphorylated PDK1, and (iii) autoinhibition of kinase activation is relieved upon binding of the PH domain to the PI(3,4,5)P₃ second messenger, which facilitates *trans*-autophosphorylation of Thr-513 in the PH domain. The results of mutagenesis studies suggest that chemical modification of residue 513 may cause dissociation of autoinhibitory contacts formed between the contiguous regulatory PH and catalytic kinase domains.

2. Materials and methods

2.1. Materials

‘Full length’ constructs (residues 51–556) of wild type and mutant PDK1s [His₆-PDK1, His₆-PDK1(T513A), His₆-PDK1(T513E), His₆-PDK1(S241A), and His₆-PDK1(S241E),

His₆-PDK1(S241E, T513A), and His₆-PDK1(S241E, T513E)], as well as the catalytic kinase domain of PDK1 [His₆-PDK1(Δ PH), residues 51–359] [21], each containing an N-terminal His₆ tag followed by a PreScission protease recognition sequence prior to residue 51, were expressed using the Bac-to-Bac[®] Baculovirus Expression System (Invitrogen, Inc., Carlsbad, CA) and His₆ affinity purified as described [20]. Mutagenesis was carried out using the QuikChange Site-Directed Mutagenesis Kit (Stratagene). Unphosphorylated wild type and mutant forms of His₆-PDK1 and His₆-PDK1(Δ PH) were generated by treatment with λ PP as described [20]. The N-terminal His₆ affinity tag was removed from purified active preparations of both His₆-PDK1 and His₆-PDK1(Δ PH) by incubation with glutathione *S*-transferase (GST)-PreScission protease (Amersham); and the cleaved enzyme product was purified simultaneously from cleaved His₆ affinity tag, uncleaved enzyme, and the GST-PreScission protease by shaking 30 min with 200 μ L of Ni-NTA agarose resin and 200 μ L of glutathione-Sepharose [38]. PDK1-Tide and T308-Tide were from 21st Century Biochemicals, Inc. (Marlboro, MA). [γ -³²P]ATP was from MP-Bio-medical (Irvine, CA). D-Myo-inositol (1,3,4,5)-tetrakisphosphate [I(1,3,4,5)P₄], D-myo-inositol (1,3,4,6)-tetrakisphosphate [I(1,3,4,6)P₄], and D-myo-inositol (1,4,5)-triphosphate [I(1,4,5)P₃] were from Sigma-Aldrich (St. Louis, MO). 1,2-Dioleoyl-*sn*-glycerol-3-phosphocholine (PC), 1,2-dioleoyl-*sn*-glycerol-3-phospho-L-serine (PS), *sn*-1-stearoyl-2-arachidonoyl D-phosphatidylinositol-(3,4,5)-triphosphate [PI(3,4,5)P₃], and *sn*-1-stearoyl-2-arachidonoyl D-phosphatidylinositol-(4,5)-bisphosphate [PI(4,5)P₂] were from Echelon Biosciences (Salt Lake City, UT).

2.2. Autophosphorylation of His₆-PDK1(Δ PH)

Varying concentrations of purified active (His₆ tag removed) PDK1(Δ PH) [1.0 μ M (0.7 mg/20 mL), 2.0 μ M (1.4 mg/20 mL), and 5 μ M (3.5 mg/20 mL)] were preincubated with 0.5 μ M (0.35 mg/20 mL) λ PP-treated unphosphorylated His₆-PDK1(Δ PH) for 5 min with continuous shaking at 30 °C in 50 mM Tris-HCl buffer, pH 7.5, containing 1 mM 2-mercaptoethanol, 10 mM MgCl₂, and 0.2 mM sodium vanadate. Autophosphorylation reactions were initiated by addition of 100 μ M [γ -³²P]ATP (~100–500 cpm/pmol). For determination of both total amounts of ³²P-radiolabeled protein and fraction amounts of site-specific phosphorylation, a 2 mL volume containing 35 μ g (1 nmol) of His₆-PDK1(Δ PH) was removed and quenched by addition of 6 mL of 8 M urea at different times. ³²P-radiolabeled His₆-PDK1(Δ PH) in the quenched reaction mixtures was His₆ affinity purified from both PDK1(Δ PH) and [γ -³²P]ATP; and the corrected specific radioactivity for site-specific phosphorylation was determined as described below. Control assays were carried out in which either (i) the reaction mixtures containing active PDK1(Δ PH) and unphosphorylated His₆-PDK1(Δ PH) were quenched before addition of [γ -³²P]ATP, (ii) unphosphorylated His₆-PDK1(Δ PH) was left out of the reaction mixture, or (iii) active PDK1(Δ PH) was left out of the reaction mixture. In addition, a kinetic time course was followed using 0.5 μ M λ PP-treated unphosphorylated His₆-PDK1(Δ PH) in the presence of 2 μ M active PDK1 (full length).

2.3. Autophosphorylation of His₆-PDK1

Varying concentrations of λ PP-treated unphosphorylated His₆-PDK1 [0.5 μ M (0.6 mg/20 mL), 2.0 μ M (0.6 mg/5.0 mL), 3.5 μ M (0.6 mg/2.86 mL), and 5 μ M (0.6 mg/2.0 mL)]

were preincubated for 5 min with continuous shaking at 30 °C in 50 mM Tris–HCl buffer, pH 7.5, containing 1 mM 2-mercaptoethanol, 10 mM MgCl_2 , and 0.2 mM sodium vanadate. Autophosphorylation reactions were initiated by addition of 100 μM $[\gamma\text{-}^{32}\text{P}]\text{ATP}$ ($\sim 100\text{--}500$ cpm/pmol). For determination of both total amounts of ^{32}P -radiolabeled protein and fraction amounts of site-specific phosphorylation, a volume containing 60 μg (1 nmol) of His₆-PDK1 was removed and quenched by addition of urea to 6 M at different times. ^{32}P -radiolabeled His₆-PDK1 in the quenched reaction mixtures was His₆ affinity purified from $[\gamma\text{-}^{32}\text{P}]\text{ATP}$; and the corrected specific radioactivity for site-specific phosphorylation was determined as described below. Control assays were carried out in which the reaction mixture containing unphosphorylated His₆-PDK1 was quenched before addition of $[\gamma\text{-}^{32}\text{P}]\text{ATP}$.

2.4. Effect of inositol phosphates and phosphoinositides on His₆-PDK1 autophosphorylation and catalytic activation

The kinetics of His₆-PDK1 autophosphorylation were carried out exactly as described above except that 50 μM of either I(1,3,4,5)P₄, I(1,3,4,6)P₄, or I(1,4,5)P₃ was included in the reaction buffer. For reactions with phosphoinositides, small unilamellar vesicles were formulated with total concentrations in the reaction mixture of 413 μM PC, 413 μM PS, and either 0, 10, 30, or 70 μM of either PI(3,4,5)P₃ or PI(4,5)P₂. The PC/PS/PIP_x phospholipid vesicles were prepared as described [20].

2.5. Progress curves for site-specific autophosphorylation

Site-specific autophosphorylation was verified at each time point for both His₆-PDK1 and His₆-PDK1(ΔPH) autophosphorylation reactions. The quenched reaction mixtures containing either 60 or 35 μg (1 nmol) of either His₆-PDK1 or His₆-PDK1(ΔPH), respectively, were affinity purified from the reaction components by addition of 200 μL of Ni-NTA agarose resin (contained in 6 M urea) and shaking overnight at room temperature. After low speed centrifugation, the supernatant was removed and the resin was washed twice with 1 mL of 50 mM Tris–HCl, pH 7.5, containing 6 M urea, 50 mM imidazole, 300 mM NaCl, and 1 mM 2-mercaptoethanol. Either His₆-PDK1 or His₆-PDK1(ΔPH) was eluted from the Ni-NTA agarose resin pellet with 100 μL of 50 mM Tris–HCl, pH 7.5, containing 6 M urea, 500 mM imidazole, 300 mM NaCl, and 1 mM 2-mercaptoethanol; and approximately 40–50% of enzyme (400–500 pmol) was recovered in the 100 μL elute for each time point. First, protein concentration was determined with the Bio-Rad protein assay kit, using 10 μL of the eluted enzyme. Second, the specific radioactivity of either His₆-PDK1 or His₆-PDK1(ΔPH) (SA^{PDK1} , cpm/pmol) was determined from radioactivity detected by scintillation counting of the known amount of enzyme ($\sim 40\text{--}50$ pmol) in 10 μL of the eluted enzyme. The concentration of phosphorylated sites was calculated by $[\text{PO}_3^{2-}] (\mu\text{M}) = (\text{SA}^{\text{PDK1}}/\text{SA}^{\text{ATP}}) \times [\text{PDK1}]_{\text{tot}} (\mu\text{M})$.

The remaining amount (~ 80 μL with $\sim 320\text{--}400$ pmol) of affinity purified His₆-PDK1 (intramolecular autophosphorylation assays) or His₆-PDK1(ΔPH) (intermolecular autophosphorylation assays) was used for trypsin digestion and HPLC resolution of ^{32}P -radiolabeled peptides to determine fractional amounts of site-specific phosphorylation. First, cysteine residues were reduced by addition of 0.5 mL of 50 mM Tris–HCl, pH 7.5, containing 20 mM 2-mercaptoethanol. Free cysteines were protected from re-oxidation by subsequent

addition of 50 μL of 500 mM iodoacetamide incubation in the dark at room temperature for 20 min. Excess unreacted iodoacetamide was depleted from the reaction mixture by further addition of 30 μL of 500 mM 2-mercaptoethanol and incubation at room temperature for 5 min. Proteolytic digestion was carried out by addition of 1 μg trypsin and incubation at 37 °C for 5 h, followed by subsequent addition of 1 μg trypsin and incubation at 37 °C overnight. The individual reaction mixtures (~ 200 μL) containing either digested ^{32}P -radiolabeled His₆-PDK1(ΔPH) or digested ^{32}P -radiolabeled His₆-PDK1 were diluted to 1 mL with solvent A [0.1% (v/v) trifluoroacetic acid in water]. The 1 mL samples were directly loaded by HPLC (0.5 mL/min) onto a $\mu\text{RPC C2/C18}$ column (Amersham) equilibrated in 100% solvent A. The column was subsequently washed in this buffer for 5 min, and the peptides were eluted by linear increasing solvent B [80% acetonitrile and 0.07% (v/v) trifluoroacetic acid in water] from 0% to 50% in 1 h at a flow rate of 0.4 mL/min, while 300 μL were collected for each fraction. ^{32}P -radiolabeled peptides were detected by scintillation counting of 30 μL of each chromatographic fraction ($\leq 12,000$ cpm).

Since phosphopeptide mapping indicated only one site of phosphorylation for both His₆-PDK1(ΔPH) and His₆-PDK1 under all conditions not including PI(3,4,5)P₃, the progress of site-specific Ser-241 autophosphorylation was given by the concentration of phosphorylated sites, as described above for $[\text{PO}_3^{2-}]$ (μM) = $(\text{SA}^{\text{PDK1}}/\text{SA}^{\text{ATP}}) \times [\text{PDK1}]_{\text{tot}}$ (μM). For His₆-PDK1 autophosphorylation in the presence of PI(3,4,5)P₃, the fractional amount of radioactivity detected for the ^{32}P -Ser-241 and ^{32}P -Thr-513 tryptic peptides were calculated according to $f_{\text{peptide}} = ^{32}\text{P-peptide}/[^{32}\text{P-Ser-241} + ^{32}\text{P-Thr-513}]$. The fractional amounts of the ^{32}P -Ser-241 and ^{32}P -Thr-513 tryptic peptides were used to determine the concentrations of mono-phosphorylated PDK1(pS241) and di-phosphorylated PDK1(pS241, pT513) in total phosphorylated PDK1 (see text).

2.6. MALDI-TOF analysis of phosphopeptides

The identities of the ^{32}P -radiolabeled peptides were confirmed by MALDI-TOF mass spectrometric analysis. The 300 μL fractions containing ^{32}P -radiolabeled peptides were evaporated to dryness and resuspended in a small volume (10–30 μL) of 50% acetonitrile to yield ^{32}P -peptide concentrations of 10 pmol/ μL , as indicated by the amount of radioactivity; 1 μL of saturated 2,5-dihydroxybenzoic acid (2,5-DHB) was added to 1 μL of the concentrated ^{32}P -peptide, and 1 μL of this mixture containing 5 pmol of the ^{32}P -peptide was placed on a stainless steel MALDI-TOF target plate and allowed to dry. MALDI-TOF mass spectra were acquired on a Biflex IV MALDI-TOF mass spectrometer (Bruker Daltronics) in either linear (larger peptides) or reflectron (smaller peptides) mode. A N₂ laser was used to desorb/ionize the matrix/analyte material. Calibration was performed using angiotensin II (monoisotopic mass $[\text{MH}^+]$ 1046.5423 Da), angiotensin I (monoisotopic mass $[\text{MH}^+]$ 1296.6900 Da), bombesin (monoisotopic mass $[\text{MH}^+]$ 1619.8229 Da), and adrenocorticotrophic hormone clip 18–39 (monoisotopic mass $[\text{MH}^+]$ 2465.2027 Da) (Sigma–Aldrich, St. Louis, MO).

2.7. Catalytic activation of His₆-PDK1 and His₆-PDK1(ΔPH)

At the end of the time courses for each of the kinetic reactions, a remaining aliquot was not quenched with urea. Rather, either His₆-PDK1 or His₆-PDK1(ΔPH) (≤ 60 μg) was affinity purified from the reaction components by addition of 200 μL of Ni–NTA agarose

resin and shaking 2 h at 4 °C. After low speed centrifugation, the supernatant was removed and the resin was washed twice with 1 mL of 50 mM Tris–HCl, pH 7.5, 50 mM imidazole, 300 mM NaCl, and 1 mM 2-mercaptoethanol. Either His₆-PDK1 or His₆-PDK1(Δ PH) were eluted with 100 μ L of 50 mM Tris–HCl, pH 7.5, containing 500 mM imidazole, 300 mM NaCl, and 1 mM 2-mercaptoethanol; and approximately 40–50% of enzyme (400–500 pmol) was recovered. First, protein concentration was determined with the Bio-Rad protein assay kit, using 10 μ L of the eluted enzyme. SDS–PAGE was used to visualize total protein by Coomassie staining, while Ser-241 phosphorylated enzyme was visualized by Western analysis with phospho-PDK1 (Ser-241) polyclonal rabbit antibody as described [20]. The catalytic activities of the purified His₆-PDK1 and His₆-PDK1(Δ PH) reaction products were determined for *trans*-phosphorylation of 100 μ M of either the T308-Tide or the PDK1-Tide model peptide substrates as described [20]. In addition, catalytic activities of purified and λ PP-treated forms of His₆-PDK1(T513A), His₆-PDK1(T513E), His₆-PDK1(S241A), and His₆-PDK1(S241E), His₆-PDK1(S241E, T513A), and His₆-PDK1(S241E, T513E) were determined for *trans*-phosphorylation of 100 μ M of either the T308-Tide or PDK1-Tide as described [20]. One unit of activity was defined as the amount of enzyme required to catalyze phosphorylation of 1 nmol of peptide substrate in 1 min.

2.8. Analytical ultracentrifugation

Sedimentation equilibrium experiments were performed by Alliance Protein Laboratories (Thousand Oaks, CA), using a Beckman–Coulter ProteomeLab XL-I analytical centrifuge equipped with both absorbance and Rayleigh interference (refractive index


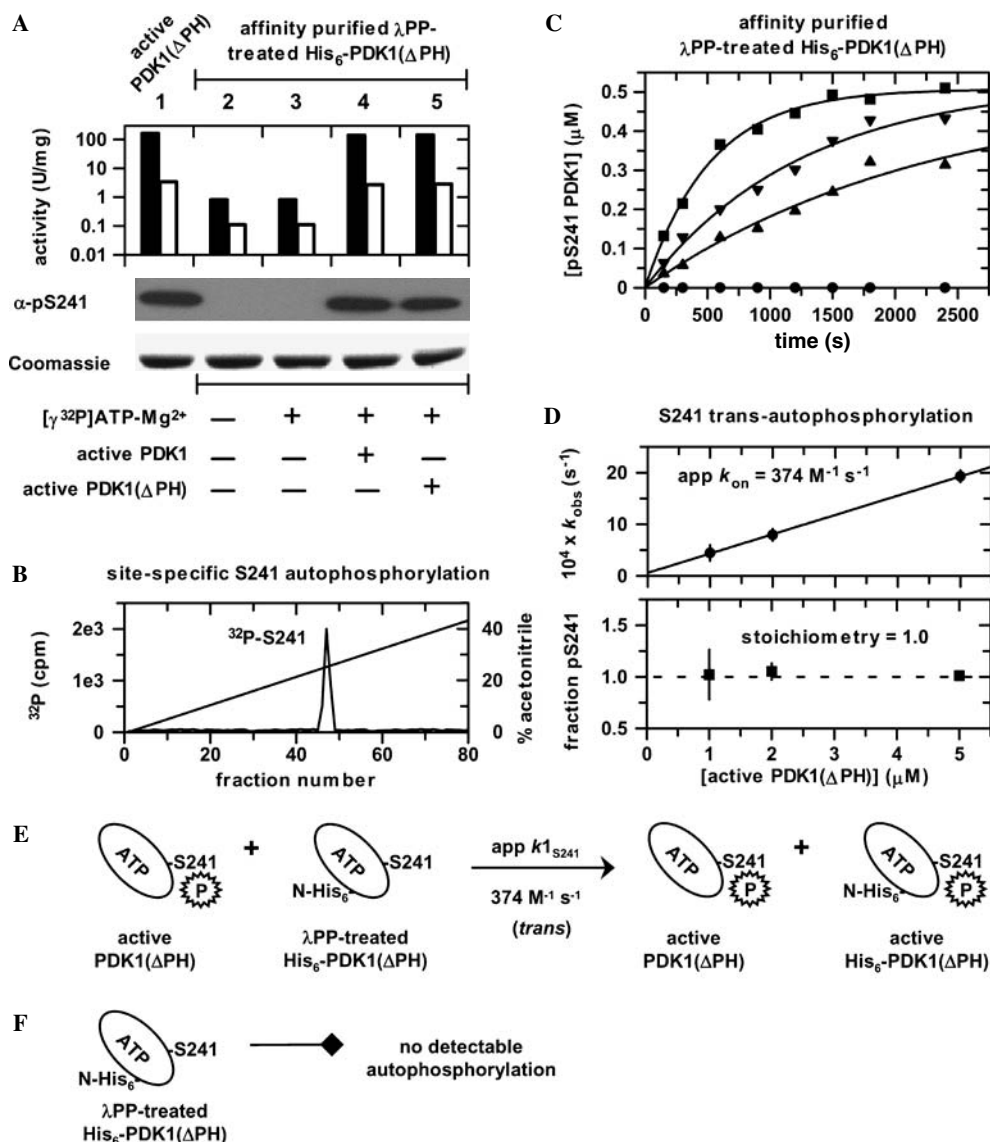


Fig. 1. Site-specific Ser-241 intermolecular autophosphorylation of λ PP-treated His₆-PDK1(Δ PH). (A) Preparation of active PDK1(Δ PH) (lane 1); preparation of λ PP-treated unphosphorylated His₆-PDK1(Δ PH) (lane 2); and affinity purified λ PP-treated His₆-PDK1(Δ PH) after 40 min incubation at 30 °C in autophosphorylation reaction mixtures containing [γ -³²P]ATP–Mg²⁺ (lane 3), [γ -³²P]ATP–Mg²⁺ in the presence of active PDK1 (lane 4), and [γ -³²P]ATP–Mg²⁺ in the presence of active PDK1(Δ PH) (lane 5). SDS–PAGE was used to visualize total protein by Coomassie staining, while Ser-241 phosphorylated enzyme was visualized by Western analysis with phospho-PDK1 (Ser-241) polyclonal rabbit antibody. Catalytic activities were determined for *trans*-phosphorylation of 100 μ M of either the PDK1-Tide (filled bars) or the T308-Tide substrates (open bars). (B) After 40 min incubation at 30 °C in the autophosphorylation reaction mixture containing [γ -³²P]ATP–Mg²⁺ in the presence of active PDK1(Δ PH), affinity purified λ PP-treated His₆-PDK1(Δ PH) was digested with trypsin and subjected to reversed-phase HPLC. Scintillation counting of the individual fractions detected a single ³²P-radiolabeled peptide that eluted at 25–26% acetonitrile, which was identified by MALDI-TOF to be the mono-phosphorylated tryptic peptide containing Ser-241. (C) 0.5 μ M λ PP-Treated His₆-PDK1(Δ PH) was reacted with 100 μ M [γ -³²P]ATP and 10 mM MgCl₂ in the absence (●) and in the presence of 1 μ M (▲), 2 μ M (▼), and 5 μ M active PDK1(Δ PH) (■). No autophosphorylation was detected for λ PP-Treated His₆-PDK1(Δ PH) alone. First-order reaction progress curves were observed for site-specific Ser-241 intermolecular autophosphorylation of λ PP-treated His₆-PDK1(Δ PH) by all concentrations of active PDK1(Δ PH). (D) The observed first-order rate constants, k_{obs} (●), increase with increasing concentrations of active PDK1(Δ PH), yielding an apparent bimolecular rate constant for intermolecular Ser-241 autophosphorylation of λ PP-treated His₆-PDK1(Δ PH) by active PDK1(Δ PH). Stoichiometric Ser-241 phosphorylation of His₆-PDK1(Δ PH) (■) was observed for all concentrations of active PDK1(Δ PH). Bars indicate SE. (E) Kinetic and phosphopeptide mapping studies indicated that active preparations of PDK1(Δ PH) catalyze site-specific Ser-241 *trans*-autophosphorylation and catalytic activation of λ PP-treated His₆-PDK1(Δ PH). (F) A model is depicted for the observation that λ PP-treated His₆-PDK1(Δ PH) showed no detectable autophosphorylation upon incubation with saturating concentrations of ATP–Mg²⁺.

detection) optical systems. Three sample channels (120 μL /each) were loaded with three different concentrations (2.5, 3.3, and 5.0 μM) of λPP -treated (unphosphorylated) His₆-PDK1 prepared in 50 mM Tris–HCl, pH 7.5, 150 mM NaCl, 10 mM MgCl₂, 0.1 mM AMPPNP, 0.1 mM EDTA, and 0.1 mM TCEP. Reference channels were loaded with 122 μL of buffer alone, and the cell was loaded into an AN60-TI rotor. Absorbance changes as a function of radial position were measured at a rotor speed of 20,000 rpm at 20 °C. The cell was scanned after 12, 16, 20, and 24 h. The software program SEDNTERP [22] was used to calculate (i) a polypeptide partial specific volume of 0.7347 mL/g at 20 °C for

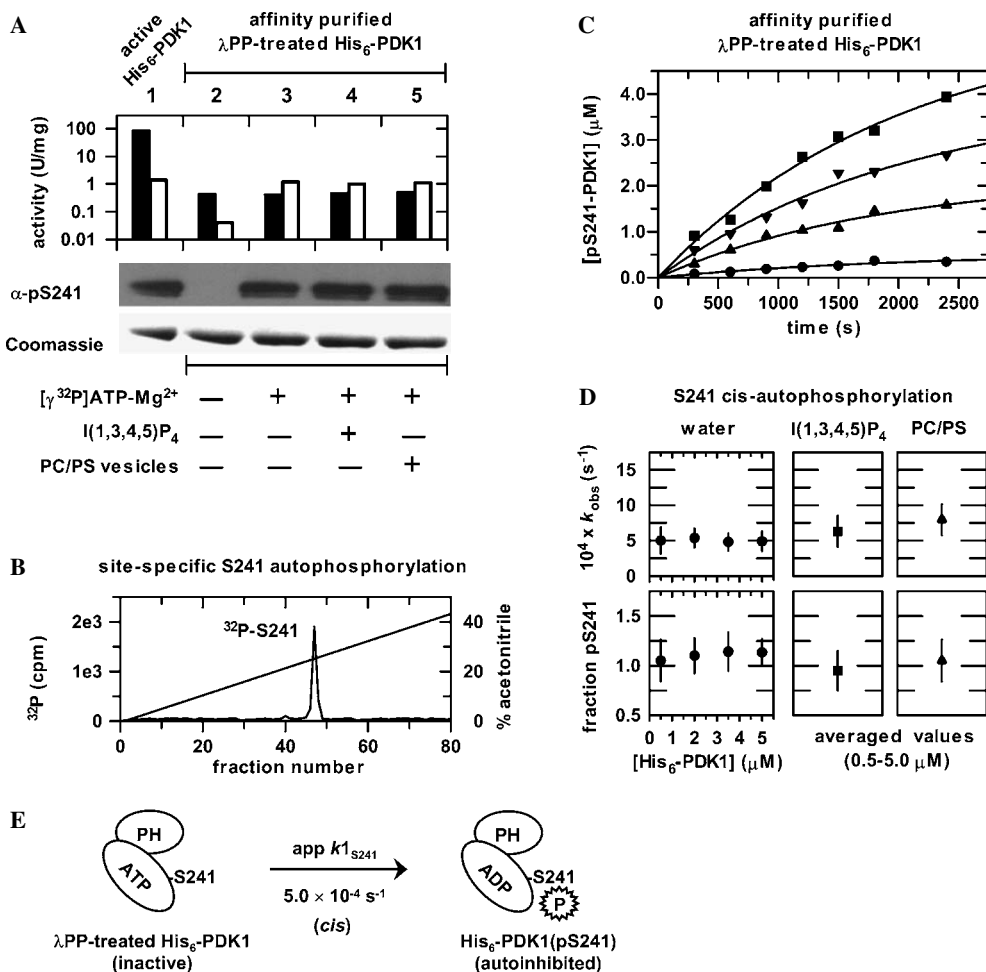


the His₆-PDK1 construct and (ii) a solvent density of 1.00653 g/mL. The resulting data were analyzed with the software program KDALTON [23,24].

3. Results

3.1. His₆-PDK1(Δ PH) requires Ser-241 trans-autophosphorylation for kinase activation

As previously reported, the recombinant catalytic domain construct of PDK1 [His₆-PDK1(Δ PH), residues 51–359] was affinity purified ($\geq 95\%$) from Sf9 insect cell lysate in its Ser-241 phosphorylated and catalytically active form [25]. Western analysis confirmed significant Ser-241 phosphorylation, and the PDK1-Tide and T308-Tide substrates were readily *trans*-phosphorylated with average catalytic activities of 165 ± 20 and 3.4 ± 0.4 U/mg, respectively (Fig. 1A, lane 1). The ~ 50 -fold higher reactivity of PDK1-Tide (**KTFCGTPEYLAPEVRREPRILSEEEQEMFRDFDYIADWC**) occurs as a result of the additional PIF residues (italic) present at the C-terminus of the T308-Tide (bold)



[25]. After treatment of His₆-PDK1(Δ PH) with λ PP for 40 min, no Ser-241 phosphorylation could be detected by Western analysis; and PDK1-Tide activity decreased 202-fold to 0.82 ± 0.41 U/mg, while T308-Tide activity decreased 30-fold to 0.11 ± 0.05 U/mg (approximate limit of detection) (Fig. 1A, lane 2).

Since recombinant His₆-PDK1(Δ PH) was purified from the Sf9 insect cells in its Ser-241 phosphorylated and catalytically active form, it seemed reasonable that the unphosphorylated isoform of His₆-PDK1(Δ PH) should have the ability to autoactivate by autocatalysis of Ser-241 phosphorylation. In order to test this possibility, 0.5 μ M of λ PP-treated unphosphorylated His₆-PDK1(Δ PH) was incubated with 100 μ M [γ -³²P]ATP and 10 mM Mg²⁺ for 40 min. Most surprisingly, Western analysis showed no detectable Ser-241 autophosphorylation, and catalytic activity of His₆-PDK1(Δ PH) to both PDK1-Tide and T308-Tide remained at the same decreased levels (Fig. 1A, lane 3). These results indicate that recombinant constructs of the catalytic domain of PDK1, whether in Sf9 insect cells or in human cells lines (e.g., HEK 293 cells), require some amount of *trans*-phosphorylation of Ser-241 by either endogenous active PDK1 or some unidentified Ser-241 kinase. In order to test this possibility, the N-terminal His₆ tag was proteolytically removed from an active preparation of the recombinant 'full length' construct of PDK1 (His₆-PDK1, residues 51–556), and a 4-fold excess amount of active PDK1 (2 μ M) was incubated with 0.5 μ M λ PP-treated unphosphorylated His₆-PDK1(Δ PH) in the presence of 100 μ M [γ -³²P]ATP and 10 mM Mg²⁺ for 40 min. His₆-PDK1(Δ PH) was affinity purified from the reaction components; and Western analysis showed that it became phosphorylated at Ser-241 and \sim 85% of its catalytic activity for *trans*-phosphorylation of both PDK1-Tide and T308-Tide was restored (Fig. 1A, lane 4).

Two possible mechanisms may be envisioned to explain how His₆-PDK1(Δ PH) undergoes Ser-241 phosphorylation upon addition of purified active PDK1. First, purified active

Fig. 2. Site-specific Ser-241 intramolecular autophosphorylation of λ PP-treated His₆-PDK1. (A) Preparation of active PDK1 (lane 1); preparation of λ PP-treated unphosphorylated His₆-PDK1 (lane 2); and affinity purified λ PP-treated His₆-PDK1 after 40 min incubation at 30 °C in autophosphorylation reaction mixtures containing [γ -³²P]ATP-Mg²⁺ (lane 3), [γ -³²P]ATP-Mg²⁺ in the presence of I(1,3,4,5)P₄ (lane 4), and [γ -³²P]ATP-Mg²⁺ in the presence of PC/PS vesicles (lane 5). SDS-PAGE was used to visualize total protein by Coomassie staining, while Ser-241 phosphorylated enzyme was visualized by Western analysis with phospho-PDK1 (Ser-241) polyclonal rabbit antibody. Catalytic activities were determined for *trans*-phosphorylation of 100 μ M of either the PDK1-Tide (filled bars) or the T308-Tide substrates (open bars). (B) After 40 min incubation at 30 °C in the autophosphorylation reaction mixture containing [γ -³²P]ATP-Mg²⁺, affinity purified λ PP-treated His₆-PDK1 was digested with trypsin and subjected to reversed-phase HPLC. Scintillation counting of the individual fractions detected a single ³²P-radiolabeled peptide that eluted at 25–26% acetonitrile, which was identified by MALDI-TOF to be the mono-phosphorylated tryptic peptide containing Ser-241. (C) Increasing concentrations of λ PP-Treated His₆-PDK1 [0.5 μ M (●), 2.0 μ M (▲), 3.5 μ M (▼), and 5.0 μ M (■)] were reacted with 100 μ M [γ -³²P]ATP and 10 mM MgCl₂. First-order reaction progress curves were observed for site-specific Ser-241 autophosphorylation at all concentrations of λ PP-treated His₆-PDK1. (D) Plots of the observed first-order rate constants (k_{obs}) and stoichiometries versus His₆-PDK1 concentration (●). Concentration independent values of k_{obs} indicate zero-order reaction kinetics with respect to Ser-241 autophosphorylation catalyzed by λ PP-treated His₆-PDK1. In addition, concentration independent values of k_{obs} or zero-order reaction kinetics were obtained with respect to λ PP-treated His₆-PDK1 (0.5 and 5.0 μ M) in the presence of either 50 μ M I(1,3,4,5)P₄ (■) or PC/PS vesicles (▲). Stoichiometric Ser-241 phosphorylation was observed for all concentrations of His₆-PDK1 in the absence and presence of either I(1,3,4,5)P₄ or PC/PS vesicles. Bars indicate SE. (E) A model is depicted whereby the C-terminal PH domain activates Ser-241 *cis*-autophosphorylation. This model is proposed on the basis of the inability to detect PDK1 self-association over this concentration range as demonstrated in Fig. 4.

PDK1 may simply *trans*-phosphorylate His₆-PDK1(Δ PH). Alternatively, the PH domain of purified active His₆-PDK1 may *trans*-activate His₆-PDK1(Δ PH) to undergo intramolecular Ser-241 autophosphorylation. Therefore, the N-terminal His tag was proteolytically removed from purified active His₆-PDK1(Δ PH); and autophosphorylation was carried out with 2 μ M active PDK1(Δ PH) and 0.5 μ M λ PP-treated unphosphorylated His₆-PDK1(Δ PH) (Fig. 1E). Upon affinity purification of His₆-PDK1(Δ PH) from active PDK1(Δ PH), Western analysis showed significant Ser-241 phosphorylation of His₆-PDK1(Δ PH) and \sim 90% of its catalytic activity for *trans*-phosphorylation of both PDK1-Tide and T308-Tide was restored (Fig. 1A, lane 5). Taken together, these results indicate a mechanism whereby purified active preparations of either PDK1 (Fig. 1A, lane 4) or PDK1(Δ PH) (Fig. 1A, lane 5) *trans*-phosphorylate Ser-241 of His₆-PDK1(Δ PH), resulting in direct and immediate catalytic activation.

In order to further investigate the kinetic mechanism, Ser-241 *trans*-autophosphorylation was followed under single turnover conditions, using different concentrations of purified active PDK1(Δ PH) (0, 1, 2 and 5 μ M) to phosphorylate a fixed concentration of λ PP-treated His₆-PDK1 (Δ PH) (0.5 μ M), using 100 μ M [γ -³²P]ATP and 10 mM Mg²⁺. At different times (0–40 min), the reactions were quenched, and His₆-PDK1(Δ PH) was affinity purified from the reaction components. Time progress curves for site-specific phosphorylation were generated by first measuring the total specific radioactivity of affinity purified His₆-PDK1(Δ PH) and then proteolytically digesting His₆-PDK1(Δ PH) with trypsin. ³²P-radiolabeled peptides were separated by reversed-phase HPLC and detected by scintillation counting of the individual fractions (Fig. 1B). For all time points that included active PDK1(Δ PH) in the reaction mixture, a single ³²P-containing peak eluted near 25–26% acetonitrile (fractions 46–48); and MALDI-TOF analysis of fraction 47 indicated a major peak with its $m/z = 2134.1$, which corresponds to the tryptic peptide (residues 239-AN $\underline{\text{S}}$ FVGTAQYVSP $\underline{\text{E}}$ LLTEK-256) containing phospho-Ser-241 [13,14]. For these reactions, Ser-241 phosphorylation increased in a single exponential manner, yielding k_{obs} values of $(4.4 \pm 1.5) \times 10^{-4}$, $(7.9 \pm 1.2) \times 10^{-4}$, and $(19.3 \pm 1.2) \times 10^{-4} \text{ s}^{-1}$ for active PDK1(Δ PH) concentrations of 1, 2, and 5 μ M, respectively (Fig. 1C). These proportionately increasing values of k_{obs} with increasing active PDK1(Δ PH) concentrations yielded an apparent bimolecular rate constant of $^{\text{app}}k_{1\text{S}241} = 374 \pm 29 \text{ M}^{-1} \text{ s}^{-1}$ (Figs. 1D and E) for Ser-241 *trans*-autophosphorylation. No ³²P-radiolabeled peptides were detected throughout the autophosphorylation time course for λ PP-treated His₆-PDK1(Δ PH) in the absence of active PDK1(Δ PH) (Fig. 1C), which further establishes that unphosphorylated His₆-PDK1(Δ PH) cannot catalyze Ser-241 autophosphorylation nor any other sites within itself (Fig. 1F).

3.2. PH domain of full length His₆-PDK1 activates apparent first-order Ser-241 autophosphorylation and autoinhibits kinase activity

As previously reported, full length His₆-PDK1 was affinity purified (\geq 95%) from Sf9 insect cell lysate in its Ser-241 phosphorylated and catalytically active form (Fig. 2A, lane 1) [20,25]. Western analysis confirmed significant Ser-241 phosphorylation, and the PDK1-Tide and T308-Tide substrates were readily *trans*-phosphorylated with average catalytic activities of 83 ± 11 and $1.4 \pm 0.2 \text{ U/mg}$, respectively. After treatment of His₆-PDK1 with λ PP for 40 min, no Ser-241 phosphorylation could be detected by Western analysis; and PDK1-Tide activity decreased 198-fold to $0.42 \pm 0.19 \text{ U/mg}$, while T308-

Tide activity decreased 35-fold to 0.04 ± 0.03 U/mg (approximate limit of detection) (Fig. 2A, lane 2).

In contrast to the isolated catalytic domain of PDK1 [His₆-PDK1(Δ PH); Fig. 1A, lane 3], Western analysis showed significant Ser-241 autophosphorylation upon incubation of $0.5 \mu\text{M}$ of λ PP-treated unphosphorylated His₆-PDK1 with $100 \mu\text{M}$ [γ -³²P]ATP and 10 mM Mg²⁺ for 40 min (Fig. 2A, lane 3). Interestingly, autophosphorylation under these conditions restored the small amount of PDK1 catalytic activity towards T308-Tide *trans*-phosphorylation, but activity towards PDK1-Tide *trans*-phosphorylation was not restored (Fig. 2A, lane 3). These data indicate that the PH domain enables unphosphorylated His₆-PDK1 to catalyze Ser-241 autophosphorylation. In addition, the observation that the PDK1-Tide activity remained similar to the restored amount of T308-Tide activity suggests that PIF interactions are autoinhibited in the Ser-241 mono-phosphorylated form of His₆-PDK1. Alternatively, the observed autoinhibition of PDK1-Tide activity could result from additional or nonspecific autophosphorylation sites, which occur subsequent to intermolecular Ser-241 autophosphorylation.

The time courses for autophosphorylation at all possible sites were followed using different concentrations of λ PP-treated His₆-PDK1 (0.5 , 2.0 , 3.5 and $5.0 \mu\text{M}$). For all time points and His₆-PDK1 concentrations, a single ³²P-containing peak eluted near 25–26% acetonitrile (fractions 46–48). A representative HPLC chromatogram is shown for the highest His₆-PDK1 concentration ($5 \mu\text{M}$) at the longest time point (40 min) (Fig. 2B); and MALDI-TOF analysis of fraction 47 indicated a major peak with $m/z = 2134.1$, which corresponds to the tryptic peptide (residues 240–256) containing phospho-Ser-241. Since a single mono-phosphorylated peptide was detected for all time and reaction conditions, the observation that the PDK1-Tide activity remained similar to the restored amount of T308-Tide activity rules out the possibility that inhibition of PDK1-Tide activity occurs as a result of additional or nonspecific autophosphorylation sites. Rather, autoinhibition of PDK1-Tide activity in the Ser-241 mono-phosphorylated form of His₆-PDK1 likely results from the inability of the catalytic kinase domain to form favorable PIF interactions with the PIF-fragment containing PDK1-Tide.

In addition to the establishment that Ser-241 mono-phosphorylated PDK1 is not fully activated, the concentration dependence of the reaction progress curves can provide evidence regarding the mechanism of site-specific Ser-241 autophosphorylation. For Ser-241 autophosphorylation in buffer alone, Fig. 2C shows single-exponential progress curves and Fig. 2D shows zero-order reaction kinetics over a 10-fold concentration range of λ PP-treated His₆-PDK1, which yielded an average apparent first-order rate constant of ${}^{\text{app}}k_{1\text{S}241} = (5.0 \pm 1.5) \times 10^{-4} \text{ s}^{-1}$ and an average stoichiometry of 1.1 ± 0.2 . The concentration independence of k_{obs} indicates that Ser-241 autophosphorylation proceeds either (i) by an intramolecular mechanism or (ii) by an intermolecular mechanism where PDK1-PDK1 binding remains saturated over this concentration range and some other step such as chemistry or a conformational change is rate limiting. An intramolecular or *cis*-autophosphorylation mechanism (Fig. 2E) is supported by the inability to detect multimeric complexes of λ PP-treated His₆-PDK1 in sedimentation equilibrium experiments for which the results are presented later in this paper. In conclusion, these data suggest that in addition to Ser-241, one or more other sites of phosphorylation are required for catalytic activation of *full length* PDK1. The phosphate group at this site(s) in active His₆-PDK1 purified from Sf9 insect cells must have been removed during treatment with λ PP.

3.3. $PI(3,4,5)P_3$ binding activates PDK1 by promoting sequential Ser-241 and Thr-513 autophosphorylation

Since the C-terminal PH domain of PDK1 has been shown to efficiently bind the membrane-bound $PI(3,4,5)P_3$ second messenger, autophosphorylation of $0.5\ \mu M$ λPP -treated His₆-PDK1 was first carried out with either $50\ \mu M$ $I(1,3,4,5)P_4$ (Fig. 2A, lane 4) or in the presence of a PC/PS vesicle membrane alone (Fig. 2A, lane 5). In both cases, Western analysis showed significant Ser-241 autophosphorylation and PDK1 activity to T308-Tide was restored; however, activity to PDK1-Tide remained suppressed. Phosphopeptide mapping indicated site-specific Ser-241 autophosphorylation for both 0.5 and $5\ \mu M$ λPP -treated His₆-PDK1 in the presence of either $I(1,3,4,5)P_4$ or PC/PS vesicles. Single-exponential progress curves and zero-order reaction kinetics were observed over this concentration range, where average apparent first-order rate constants of $^{app}k_{1S241} = (6.3 \pm 2.2) \times 10^{-4}\ s^{-1}$ and $^{app}k_{1S241} = (7.9 \pm 2.4) \times 10^{-4}\ s^{-1}$ and average stoichiometric values of 0.95 ± 0.21 and 1.1 ± 0.2 were obtained for Ser-241 autophosphorylation in the presence of either $I(1,3,4,5)P_4$ or PC/PS vesicles, respectively (Fig. 2D). Similar values of first-order rate constants with zero-order reaction kinetics were also obtained for incubation of His₆-PDK1 with either $I(1,3,4,6)P_4$, $I(1,4,5)P_3$, or PC/PS/ $PI(4,5)P_2$ vesicles, and PDK1-Tide activity remained suppressed (data not shown).

In contrast to the site-specific Ser-241 autophosphorylation observed in the presence of either $I(1,3,4,5)P_4$ or PC/PS vesicles alone, the specific radioactivity of λPP -treated His₆-PDK1 increased ~ 2 -fold when autophosphorylation was carried out in the presence of PC/PS vesicles containing $PI(3,4,5)P_3$. Therefore, the time courses for site-specific autophosphorylation were followed using three different concentrations of λPP -treated His₆-PDK1 (0.5 , 2 , and $5\ \mu M$) and a total $PI(3,4,5)P_3$ concentration of $30\ \mu M$ (Figs. 3A–C). For each concentration of His₆-PDK1, Figs. 3D–F show HPLC resolution of two ^{32}P -radiolabeled tryptic peptides that are formed during the course of the reaction. For all His₆-PDK1 concentrations, only the ^{32}P -radiolabeled tryptic peptide containing

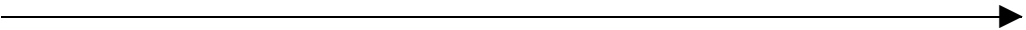
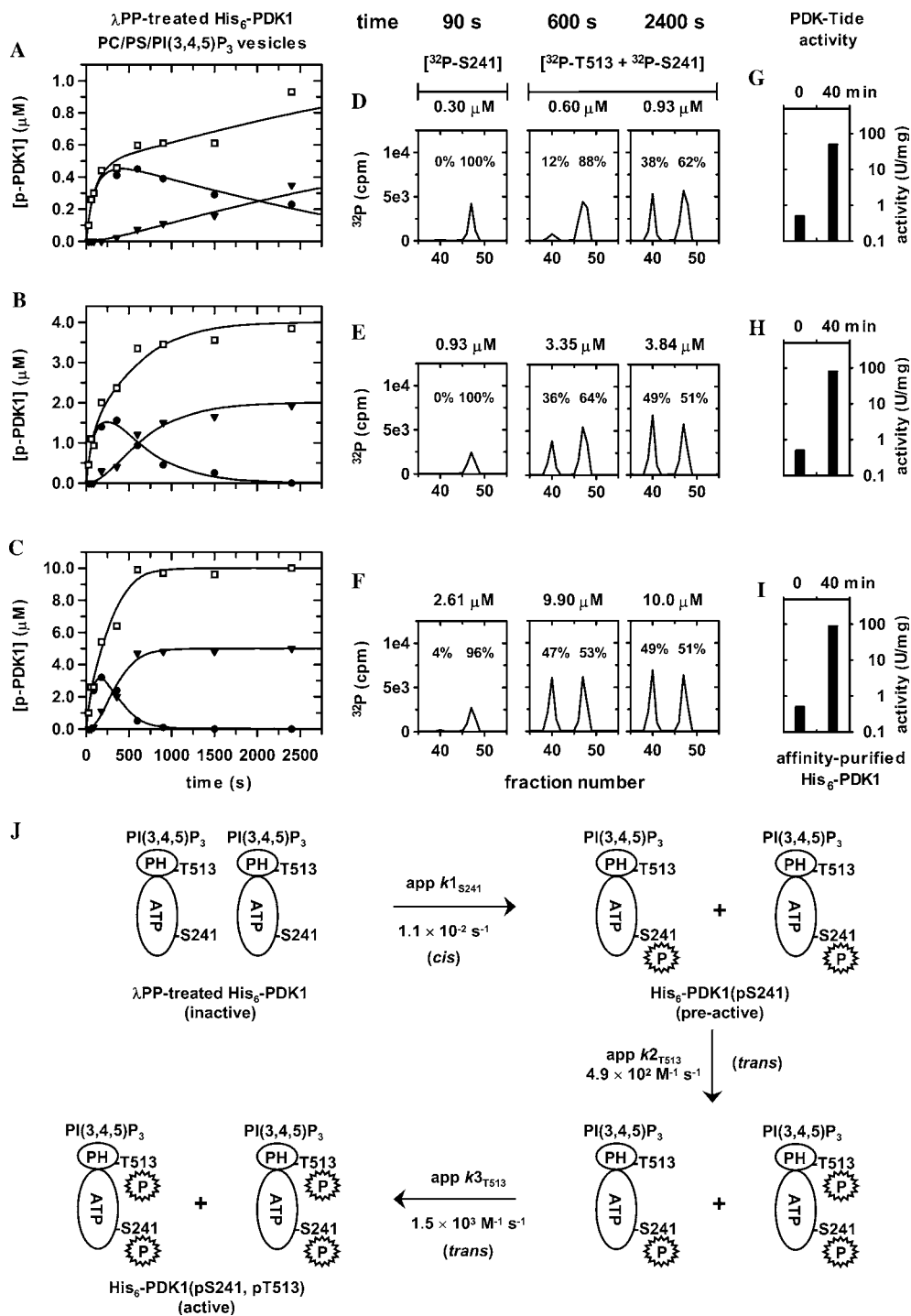


Fig. 3. Site-specific intramolecular Ser-241 and intermolecular Thr-513 autophosphorylation and catalytic activation of λPP -treated His₆-PDK1 upon binding PC/PS/ $PI(3,4,5)P_3$ vesicles. (A–C) For autophosphorylation reactions containing (A) $0.5\ \mu M$, (B) $2\ \mu M$, and (C) $5\ \mu M$ λPP -treated His₆-PDK1, time progress curves are shown for total phosphorylation (\square), appearance and disappearance of mono-phosphorylated His₆-PDK1(pS241) (\bullet), and appearance of di-phosphorylated His₆-PDK1(pS241, pT513) (\blacktriangledown). (D–F) For autophosphorylation reactions containing (D) $0.5\ \mu M$, (E) $2\ \mu M$, and (F) $5\ \mu M$ λPP -treated His₆-PDK1, the total amount of phosphorylation at each time point was determined from the specific radioactivity of affinity purified λPP -treated His₆-PDK1; and the amounts of mono-phosphorylated His₆-PDK1(pS241) and di-phosphorylated His₆-PDK1(pS241, pT513) were determined from the fractional amounts of radioactivity detected for the ^{32}P -Ser-241 and ^{32}P -Thr-513 containing peptides, which were resolved by reversed-phase HPLC after digestion with trypsin (see text). (G–I) For autophosphorylation reactions containing (G) $0.5\ \mu M$, (H) $2\ \mu M$, and (I) $5\ \mu M$ λPP -treated His₆-PDK1, catalytic activities were determined for *trans*-phosphorylation of $100\ \mu M$ of PDK1-Tide before and after 40 min autophosphorylation. (J) In the presence of PC/PS vesicles containing the $PI(3,4,5)P_3$ membrane-bound second messenger, a minimum of three different autophosphorylation reactions are required to generate fully active PDK1 from unphosphorylated PDK1. First, unphosphorylated PDK1 is recruited to bind to $PI(3,4,5)P_3$, where unphosphorylated PDK1 catalyzes apparent first-order Ser-241 autophosphorylation. Second, mono-phosphorylated PDK1(pS241) catalyzes slow intermolecular Thr-513 autophosphorylation of mono-phosphorylated PDK1(pS241) to form di-phosphorylated PDK1(pS241, pT513). Third, di-phosphorylated PDK1(pS241, pT513) catalyzes fast intermolecular Thr-513 autophosphorylation of all remaining mono-phosphorylated PDK1(pS241), ultimately yielding fully active di-phosphorylated PDK1(pS241, pT513).



phospho-Ser-241 (fractions 46–48 at 25–26% acetonitrile) was initially detected during the first 90 s. The similar timescale for the rapid burst of Ser-241 phosphorylation over the 10-fold PDK1 concentration range is again consistent with either (i) an intramolecular mechanism or (ii) an intermolecular mechanism where PDK1-PDK1 binding remains saturated over this concentration range and some other step such as chemistry or a conformational change is rate limiting.

After ~90 s, the second ^{32}P -containing fraction began to elute near 21–22% acetonitrile (fractions 39–41); and MALDI-TOF analysis of fraction 40 indicated a major peak with $m/z = 1586.2$, corresponding to the tryptic peptide containing phospho-Thr-513 (residues 510-NFKTFFVHTPNR-521). No ^{32}P -radiolabeled peaks were detected for the shorter tryptic peptide containing phospho-Thr-513 (residues 513-TFFVHTPNR-521), indicating that the peptide bond between Lys-512 and phospho-Thr-513 was not hydrolyzed by trypsin. The subsequent appearance of phospho-Thr-513 occurs more rapidly with increasing concentrations of λPP -treated His₆-PDK1 used in the assay, suggesting an intermolecular mechanism; and both Ser-241 and Thr-513 eventually become stoichiometrically phosphorylated, whereby each site approaches ~50% of total amount of detected phosphate (Figs. 3D–F). Most interestingly, the catalytic activity to PDK1-Tide activity was restored ~85% in affinity purified di-phosphorylated His₆-PDK1(pS241, pT513) (Figs. 3G–I). The X-ray structure of the PH domain of PDK1 shows that Thr-513 is exposed to solvent and is located at the end of the loop immediately preceding β -sheet 6 [11]. Since Ser-241 phosphorylation alone is sufficient to activate His₆-PDK1(ΔPH) (Fig. 1), but not full length His₆-PDK1 (Fig. 2), it is likely that phosphorylation of Thr-513 is required to relieve auto-inhibition caused by the PH domain.

3.4. Kinetic model for autoregulation of PDK1 activity

The effects of the $\text{PI}(3,4,5)\text{P}_3$ second messenger on the autophosphorylation events leading to catalytic activation of PDK1 are most consistent with a kinetic model consisting of three different reaction steps (Fig. 3J): (i) fast first-order Ser-241 autophosphorylation given by the apparent first-order rate constant, $^{\text{app}}k_{1\text{S}241}$ (s^{-1}); (ii) slow intermolecular Thr-513 autophosphorylation catalyzed by mono-phosphorylated PDK1(pS241) given by the apparent bimolecular rate constant, $^{\text{app}}k_{2\text{T}513}$ ($\text{M}^{-1} \text{s}^{-1}$); and (iii) fast intermolecular Thr-513 autophosphorylation catalyzed by di-phosphorylated PDK1(pS241, pT513) given by the apparent bimolecular rate constant, $^{\text{app}}k_{3\text{T}513}$ ($\text{M}^{-1} \text{s}^{-1}$). First, it is assumed that no mono-phosphorylated PDK1(pT513) is formed during the course of the reaction. This is supported by the fact that no ^{32}P -Thr-513 peptide is detected until times where a significant amount of the ^{32}P -Ser-241 peptide has already been generated (Figs. 3D–F). Second, the use of the apparent bimolecular rate constants, $k_{2\text{T}513}$ and $k_{3\text{T}513}$, assumes that protein–protein binding is rate limiting for intermolecular Thr-513 autophosphorylation by both mono-phosphorylated PDK1(pS241) and di-phosphorylated PDK1(pS241, pT513). This is supported by appearance of the ^{32}P -Thr-513 peptide at earlier times on increasing PDK1 concentration (Figs. 3D–F). In addition, rate limiting protein–protein binding over the 0.5–5.0 μM PDK1 concentration range is consistent with this range being well below the $K_{\text{m}} = 65\text{--}80 \mu\text{M}$, reported for the optimized PDK1-Tide substrate [20,25].

At each time point, three data sets were analyzed for each PDK1 concentration (Figs. 3A–C): (i) appearance of total phospho-PDK1; (ii) appearance and disappearance of mono-phosphorylated PDK1(pS241); and (iii) appearance of di-phosphorylated

PDK1(pS241, pT513). The concentration of total phospho-PDK1 was determined from the specific radioactivity of His₆-PDK1; the concentration of di-phosphorylated PDK1(pS241, pT513) was determined from the fractional amount of total phospho-PDK1 containing the ³²P-Thr-513 peptide; and the concentration of mono-phosphorylated PDK1(pS241) was calculated from the fractional amount of total phospho-PDK1 containing the ³²P-Ser-241 peptide by subtracting the fractional amount of any di-phosphorylated PDK1(pS241, pT513) at the given time point. Global fitting of all three progress curves for the three different PDK1 concentrations using the KINSIM/FITSIM software [26] yielded values of (i) $^{app}k_{1S241} = (1.1 \pm 0.1) \times 10^{-2} \text{ s}^{-1}$ for first-order Ser-241 autophosphorylation; (ii) $^{app}k_{2T513} = (4.9 \pm 1.1) \times 10^2 \text{ M}^{-1} \text{ s}^{-1}$ for intermolecular Thr-513 autophosphorylation catalyzed by mono-phosphorylated PDK1(pS241); and (iii) $^{app}k_{3T513} = (1.5 \pm 0.2) \times 10^3 \text{ M}^{-1} \text{ s}^{-1}$ for intermolecular Thr-513 autophosphorylation catalyzed by di-phosphorylated PDK1(pS241, pT513) (Fig. 3J).

Systematic deviations of fitted curves from the data, as well as significantly higher errors, were obtained upon global fitting of the data in Fig. 3 to alternative mechanisms including: (i) all other possible three step mechanisms resulting from permutation of the kinetic order of each reaction step [e.g., $k_{1S241}(\text{M}^{-1} \text{ s}^{-1})$: $k_{2T513}(\text{M}^{-1} \text{ s}^{-1})$: $k_{3T513}(\text{M}^{-1} \text{ s}^{-1})$, $k_{1S241}(\text{M}^{-1} \text{ s}^{-1})$: $k_{2T513}(\text{M}^{-1} \text{ s}^{-1})$: $k_{3T513}(\text{s}^{-1})$, $k_{1S241}(\text{M}^{-1} \text{ s}^{-1})$: $k_{2T513}(\text{s}^{-1})$: $k_{3T513}(\text{M}^{-1} \text{ s}^{-1})$, $k_{1S241}(\text{s}^{-1})$: $k_{2T513}(\text{s}^{-1})$: $k_{3T513}(\text{M}^{-1} \text{ s}^{-1})$, $k_{1S241}(\text{s}^{-1})$: $k_{2T513}(\text{M}^{-1} \text{ s}^{-1})$: $k_{3T513}(\text{s}^{-1})$, $k_{1S241}(\text{s}^{-1})$: $k_{2T513}(\text{s}^{-1})$: $k_{3T513}(\text{s}^{-1})$, and (ii) all simplified versions of these permutations where k_{2T513} and k_{3T513} were assumed to be equal. In addition, no significant changes in the values of $^{app}k_{1S241}$, $^{app}k_{2T513}$, and $^{app}k_{3T513}$ were observed upon varying the total PI(3,4,5)P₃ concentration over 10–71 μM .

3.5. Sedimentation equilibrium experiments

The concentration independence of the observed first-order rate constant for Ser-241 autophosphorylation may result from either (i) an intramolecular mechanism or (ii) an intermolecular mechanism where PDK1–PDK1 binding remains saturated over the 0.5–5 μM concentration range (Figs. 2 and 3). In order to further address this issue, the ability of λPP -treated His₆-PDK1 (5 μM) to self-associate was examined by sedimentation equilibrium (Fig. 4). To better approximate or assist potential complex formation, the experiment was carried out in the presence of AMPPNP-Mg²⁺ using three different concentrations of λPP -treated His₆-PDK1 within the concentration range of the kinetic experiments (Figs. 2 and 3). Scans recorded at 12, 16, 20, and 24 h were superimposable, indicating that equilibrium was achieved at 12 h. The scans at 24 h were used for the data analysis. Fig. 4A shows that global single ideal species fitting of the three enzyme concentrations yields a molecular mass of $M_w = 59.4 \pm 1.2 \text{ kDa}$. This value \pm S.E. agrees well with the predicted molecular mass of monomeric unphosphorylated His₆-PDK1 construct (60,058 Da). In order to better observe whether systematic variation of M_w occurs as a function of enzyme concentration, the raw data in Fig. 4A were transformed into a plot of M_w versus enzyme concentration (Fig. 4B). In this analysis, the curvature through small groups of data points (Fig. 4A) is used to calculate M_w for average enzyme concentrations distributed across the cell (Fig. 4B). For all three loading concentrations, this graphical analysis shows no clear pattern of variation with enzyme concentration that would indicate either self-association (increasing M_w with concentration) or significant solution non-ideality (decreasing apparent M_w with concentration). The inability to detect

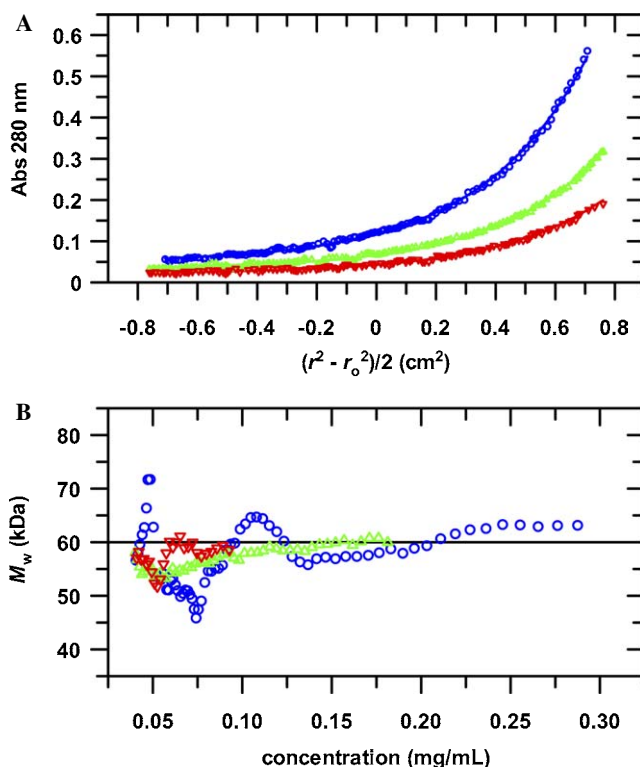


Fig. 4. Sedimentation Equilibrium Studies of λ PP-Treated PDK1. (A) Overlay of experimental data (symbols) with a global fit as a single ideal species of 59.4 kDa (lines). Colors indicate loading concentrations of λ PP-treated His₆-PDK1 of 5 μ M (blue), 3.3 μ M (green), and 2.5 μ M (red). (B) Local weight-average molecular mass, M_w , versus enzyme concentration plot calculated from the data for all three loading concentrations (using groups of 20 data points). The horizontal line marks the predicted sequence mass of the monomer. Variations observed at very low concentrations are due to low signal to noise ratio. (For interpretation of color in this figure, reader is referred to the web version of this article.)

self-associating PDK1 species in this concentration range is consistent with concentration independent S241 autophosphorylation occurring by an intramolecular or *cis* mechanism (Figs. 2 and 3).

3.6. Mutagenesis studies of the role of Ser-241 and Thr-513 in PDK1 catalytic activation

To further investigate the proposed roles of Ser-241 and Thr-513 phosphorylation in modulating the catalytic activity of PDK1, single mutant [His₆-PDK1(T513A), His₆-PDK1(T513E), His₆-PDK1(S241A), His₆-PDK1(S241E)] and double mutant [His₆-PDK1(S241E, T513A), and His₆-PDK1(S241E, T513E)] constructs were generated, expressed, and purified from Sf9 insect cells. Each mutant construct displayed comparable high levels of both expression and degree of purification as wild type His₆-PDK1 [20]. The catalytic activities to the T308-Tide (Fig. 5A) and the PDK1-Tide (Fig. 5B) are shown for each of these mutants as they were purified from Sf9 insect cells (solid bars) and after treatment with λ PP (open bars). The rationale behind such mutagenesis experiments is that

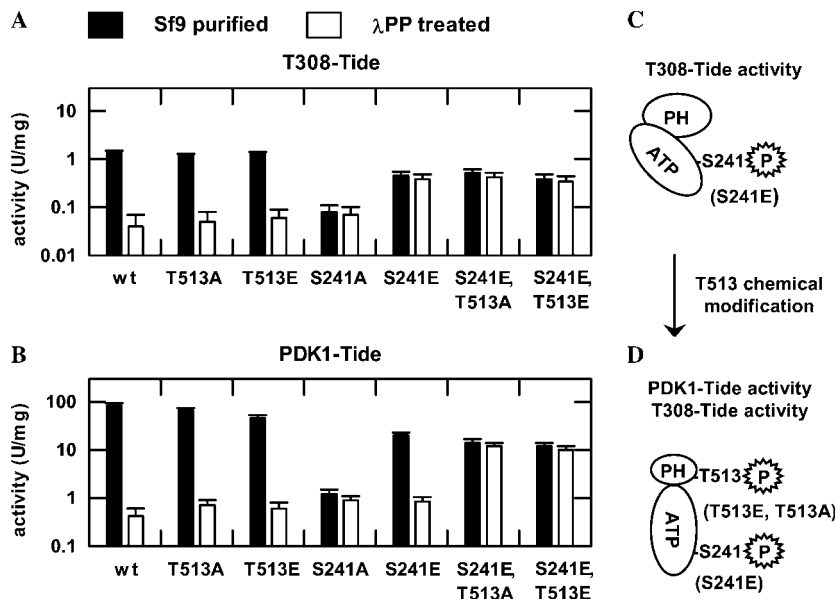


Fig. 5. Effect of Ser-241 and Thr-513 mutations on His₆-PDK1 catalytic activities to (A) T308-Tide and (B) PDK1-Tide substrates (100 μM). Catalytic activities were determined for each mutant as purified from Sf9 insect cells (filled bars) and after treatment with λPP (open bars). (C) To gain catalytic activity to the shorter T308-Tide substrate, PDK1 minimally requires a negative charge at residue 241. (D) To gain catalytic activity to the longer PDK1-Tide substrate, PDK1 requires a negative charge at residue 241, but also requires chemical modification at residue 513, which may function to destabilize autoinhibitory contacts between the contiguous regulatory PH and catalytic kinase domains.

mutation to either alanine or glutamate should mimic either the unphosphorylated or phosphorylated form of the given residue, respectively.

Compared to wild type His₆-PDK1 (T308-Tide activity = 1.4 ± 0.1 U/mg and PDK1-Tide activity = 83 ± 11 U/mg), His₆-PDK1(T513A) showed 93% and 80% of T308-Tide (Fig. 5A) and PDK1-Tide activities (Fig. 5B), respectively; and His₆-PDK1(T513E) showed 86% and 55% of T308-Tide and PDK1-Tide activities, respectively. Treatment of both His₆-PDK1(T513A) and His₆-PDK1(T513E) with λPP reduced activity levels comparable to wild type (T308-Tide activity = 0.04 ± 0.03 U/mg and PDK1-Tide activity = 0.42 ± 0.19 U/mg). That both His₆-PDK1(T513A) and His₆-PDK1(T513E) retained $\geq 86\%$ T308-Tide activity is consistent with the similar amounts of T308-Tide activity observed in purified His₆-PDK1 and reconstituted mono-phosphorylated His₆-PDK1(pS241) [Fig. 2A, lanes 1 and 3 (open bars)]. However, the higher levels of PDK1-Tide activity observed for His₆-PDK1(T513A) compared to His₆-PDK1(T513E) do not seem to be consistent with the difference in PDK1-Tide activity levels observed between reconstituted mono-phosphorylated His₆-PDK1(pS241) [Fig. 2A, lane 3 (solid bar)] and reconstituted di-phosphorylated His₆-PDK1(pS241, pT513) [Figs. 3G-I, (40 min)]. In this case, the high activity of His₆-PDK1(T513A) can only be reconciled if the alanine mutation does not truly mimic the Thr-513 unphosphorylated 'PDK1-Tide autoinhibited' state, but actually causes a structural perturbation resembling the Thr-513 phosphorylated state.

In order to address this issue, mutations at Thr-513 were further analyzed in conjunction with mutations at Ser-241. As expected, purified His₆-PDK1(S241A) exhibited decreased T308-Tide (Fig. 5A) and PDK1-Tide activities (Fig. 5B) similar to those of λ PP-treated wild type His₆-PDK1; and His₆-PDK1(S241A) activity levels were not further decreased by λ PP treatment. In this case, the S241A emulation of the low catalytic activity of the Ser-241 unphosphorylated form of PDK1 provides good indication of the absolute requirement for Ser-241 phosphorylation in PDK1 catalytic activation. Likewise, purified His₆-PDK1(S241E) emulated the Ser-241 phosphorylated and activated state of PDK1, although with somewhat reduced catalytic activities to T308-Tide (Fig. 5A, 32% of wild type) and PDK1-Tide (Fig. 5B, 24% of wild type). While λ PP treatment of purified His₆-PDK1(S241E) caused little or no loss of activity towards T308-Tide, it significantly reduced PDK1-Tide activity, indicating that a phosphate group was removed from the enzyme that is required for PDK1-Tide activity.

To further test whether the activating phosphate could have been removed from Thr-513 of His₆-PDK1(S241E), the PDK1-Tide activities were measured for the purified and λ PP-treated forms of the His₆-PDK1(S241E, T513A) and His₆-PDK1(S241E, T513E) double mutants (Fig. 5B). While the purified forms of both His₆-PDK1(S241E, T513A) and His₆-PDK1(S241E, T513E) retained PDK1-Tide activities similar to purified His₆-PDK1(S241E), λ PP treatment failed to reduce PDK1-Tide activity in either His₆-PDK1(S241E, T513A) and His₆-PDK1(S241E, T513E). These data suggest that the decreased PDK1-Tide activity observed upon treatment of His₆-PDK1(S241E) with λ PP occurs due to loss of phosphate at Thr-513. Consistent with the high PDK1-Tide activities observed in the Sf9-purified forms of both His₆-PDK1(T513A) and His₆-PDK1(T513E), the observed λ PP-resistant PDK1-Tide activity in both His₆-PDK1(S241E, T513A) and His₆-PDK1(S241E, T513E) further support the notion that Thr-513 phosphorylation may cause dissociation of autoinhibitory contacts formed between the contiguous regulatory PH and catalytic kinase domains rather than be required to participate in a specific activating salt bridge (Figs. 5C and D).

4. Discussion

4.1. Cellular circuitry and 'bio'-logic controls

An emerging view in modern cell biology is that protein kinase signaling cascades in response to extracellular stimuli rarely occur in simple linear fashion. Rather, signal transduction pathways are actually highly interconnected networks, which may be envisioned as a molecular 'circuitry' designed to precisely control cellular behavior. In a manner analogous to the use of digital logic gates (e.g., AND, OR, and NOT) to control transistor output in complex electronic circuitry, many protein kinases possess regulatory subunits or contiguous regulatory domains, which integrate multiple chemical signaling 'inputs' to precisely control their 'output' catalytic kinase activity. The concept that multi-domain signaling proteins possess such modular logic has been framed for the SH2 and SH3-containing family of Src family kinases, the SH2-containing phosphatase-2, cyclin dependent kinase-2, and N-WASP [27,28]. In each case, intramolecular interactions block a recognition event or a catalytic activity. The degree of autoinhibition rests in the relative stability or free energy difference between the inactive and active protein conformations; and chemical binding or covalent modifications provide 'allosteric' activation by altering the relative

stabilities of inactive and active protein conformations [29–31]. Such quantitative descriptions of how such signaling proteins utilize chemical ‘inputs’ to gauge control of their catalytic or functional ‘outputs’ are central to blueprint development of cellular circuitry.

The results of our kinetic studies of the phosphorylation events that lead to catalytic activation of both His₆-PDK1(Δ PH) and His₆-PDK1 provide unique and further insight towards advancing the concept of ‘bio’-logic in cellular circuitry. For PDK1 activation, the key regulatory ‘switch’ occurs at a stage where autoinhibition of the Ser-241 mono-phosphorylated isoform (Fig. 2E) is relieved upon binding of the PH domain to PI(3,4,5)P₃ so that Thr-513 can be *trans*-phosphorylated (Fig. 3J, ^{app}*k*_{2T513}). The noncovalent interaction between the PH domain and PI(3,4,5)P₃ may be considered as the ‘input’ signal that switches the conformational equilibria in favor of the active state, while Thr-513 phosphorylation may be considered as an imposed ‘lock’ that destabilizes the autoinhibited conformation.

The energetic magnitude of the conformational switch produced through PI3K-dependent signaling can be calculated from the Ser-241 and Thr-513 autophosphorylation reaction rate enhancements provided by PI(3,4,5)P₃ binding to the PH domain. First, PI(3,4,5)P₃ binding caused a 22-fold rate enhancement in the first-order Ser-241 *cis*-autophosphorylation rate constant [i.e., *k*_{1S241} increased from $5.0 \times 10^{-4} \text{ s}^{-1}$ (Fig. 2E) to $1.1 \times 10^{-2} \text{ s}^{-1}$ (Fig. 3J)] corresponding to an activation free energy difference of 1.9 kcal/mol. However, the greatest energetic contribution was observed where PI(3,4,5)P₃ binding enabled *trans*-phosphorylation of Thr-513 within a transient dimer complex of mono-phosphorylated PDK1(pS241). On the basis of the calculated limit of detection where this reaction could not be detected in the absence of PI(3,4,5)P₃ (Fig. 2), the conservative estimate of ≥ 490 -fold rate enhancement provided by PI(3,4,5)P₃ binding (Fig. 3) corresponds to an activation free energy difference of ≥ 3.8 kcal/mol. Although intermolecular Thr-513 phosphorylation of PDK1(pS241) by PDK1(pS241, pT513) occurred ~ 3 -fold faster (Fig. 3J, ^{app}*k*_{3T513}), this reaction readily occurs in the absence of PI(3,4,5)P₃ [31–34] and is consistent with the notion that chemical modification of Thr-513 mimics the conformational switch provided by PI(3,4,5)P₃ binding.

4.2. Regulation of PDK1 by reversible Thr-513 phosphorylation?

In vivo metabolic ³²P-labeling experiments of recombinant PDK1 in HEK 293 cells showed that Ser-25, Ser-241, Ser-393, Ser-396, and Ser-410 undergo a small amount of phosphorylation after a period of serum starvation [13]. Upon stimulation of these cells with growth factor, no changes were observed either in the phosphorylation pattern or in PDK1 catalytic activity, suggesting that PDK1 is not subject to regulation by reversible phosphorylation. The observation that in vivo ³²P-metabolic labeling of Thr-513 could not be detected suggests that (i) recombinant PDK1 becomes quantitatively phosphorylated at this position before introduction of ³²P-inorganic phosphate to the cell media and (ii) phospho-Thr-513 of recombinant PDK1 does not readily undergo dephosphorylation by endogenous phosphatases under transient expression conditions in the cell [13–16]. Thus, quantitative Thr-513 phosphorylation would explain constitutive activation of PDK1 in both unstimulated and stimulated HEK 293 cells.

The observation that λ PP-treated unphosphorylated His₆-PDK1 (full length) catalyzes first-order Ser-241 *cis*-autophosphorylation, but remains in an autoinhibited form in the

absence of $\text{PI}(3,4,5)\text{P}_3$ (Fig. 2E), raises the question of how Thr-513 *trans*-autophosphorylation and catalytic activation of His₆-PDK1 occurs during transient expression of recombinant PDK1 constructs. In such cases, transfection of recombinant PDK1-containing expression plasmids is carried out while cells are in enriched growth media (~24 h). During this time, conditions are favorable for initial amounts of recombinant mono-phosphorylated PDK1(pS241) to undergo Thr-513 *trans*-autophosphorylation either rapidly by a PI3K-dependent manner (Fig. 3J, $^{\text{app}}k_{1\text{S}241}$) or slowly by endogenous amounts of active PDK1 in the absence of $\text{PI}(3,4,5)\text{P}_3$ [14–17]. In either case, only a small amount of active di-phosphorylated PDK1(pS241, pT513) is required to initiate exponential propagation of Thr-513 phosphorylation throughout newly expressed PDK1, even during periods of prolonged starvation. Exponential propagation of Thr-513 *trans*-autophosphorylation would be facilitated by the principle of mass action, where the effective concentrations of recombinant mono-phosphorylated PDK1(pS241) and active di-phosphorylated PDK1(pS241, pT513) far exceed those under physiological conditions, thus driving the bimolecular reaction to completion. In addition, excessive amounts of recombinant PDK1 may preclude proper localization in the HEK 293 cells so that phospho-Thr-513 is protected from small amounts of a particular endogenous phosphatase.

While PDK1 was shown to incorporate small amounts of ^{32}P -phosphate at Ser-25, Ser-241, Ser-393, Ser-396, and Ser-410 during *in vivo* metabolic labeling of HEK 293 cells [13], recombinant PDK1 purified from these cells was shown to further incorporate small amounts of ^{32}P -phosphate at Thr-33, Ser-241, Ser-410, Thr-513 [14]. It is likely that only upon cell lysis can these residues undergo partial dephosphorylation, enabling *in vitro* autophosphorylation at these sites in the purified PDK1. Since it was necessary to use the more stable His₆-PDK1 (residues 51–556) construct, where the N-terminus was deleted, it was not possible to evaluate Ser-25 and/or Thr-33 phosphorylation. While our kinetic and mutagenesis studies indicate direct catalytic roles for Ser-241 and Thr-513 autophosphorylation, no Ser-410 autophosphorylation could be detected for all autophosphorylation assays with λPP -treated unphosphorylated His₆-PDK1. While the function of this site remains unclear, autophosphorylation of this site must require PDK1 to be phosphorylated at a site other than Ser-241 and Thr-513. Alternatively, the N-terminus may play a role in Ser-410 autophosphorylation. Nevertheless, reconstitution of PDK1 catalytic activity does not require either Ser-410 phosphorylation or the N-terminus, which is consistent with mutagenesis studies, where the S410A mutation showed no effect on catalytic activity [13]. Although Ser-396 phosphorylation is also not required for catalytic activity [13], it has been shown to be required for nuclear shuttling of PDK1 and requires phosphorylation by an unknown kinase [17].

Taken together, it should be recognized that current methods for studying protein kinase signaling in the cell (e.g., transient overexpression of target kinase) may be subject to anomalous outcomes, especially in cases where catalytic activation of a protein kinase depends on intermolecular autophosphorylation events (e.g., PDK1). In such cases, it proves highly useful to establish the chemical and mechanistic properties that specifically lead to catalytic activation. For PDK1, the *in vitro* kinetic studies clearly indicated the specific effect that $\text{PI}(3,4,5)\text{P}_3$ binding to the PH domain has on promoting sequential intramolecular Ser-241 and intermolecular Thr-513 PDK1 autophosphorylation, which gave the minimum chemical and kinetic requirements for generating catalytic activity. The kinetic models in Figs. 2E and 3J raise the very important possibility that PDK1 could be regulated by reversible Thr-513 phosphorylation under physiological conditions.

Only recently has the *PH* domain leucine-rich repeat protein phosphatase (PHLPP) been identified that preferentially dephosphorylates Ser-373 in the C-terminal hydrophobic motif of PKB α [32]. A custom phospho-specific PDK1 pT513 antibody is being generated to examine the proposed regulatory role of second messenger induced Thr-513 autophosphorylation.

4.3. Intermolecular and/or intramolecular Ser-241 autophosphorylation

Two different in vivo ^{32}P -metabolic labeling studies have been reported where autophosphorylation sites were compared between an active form of PDK1 and a kinase-defective mutant of PDK1 (PDK1^{KD}). In both cases, transiently-expressed PDK1^{KD} showed similar levels to active PDK1 in ^{32}P incorporation at either Ser-241 in human PDK1 [13] or Ser-244 in mouse PDK1 [16], certainly indicating that PDK1^{KD} was *trans*-phosphorylated by some endogenous kinase. It was further shown that active mouse PDK1 can *trans*-phosphorylate mouse PDK1^{KD} in vitro suggesting that the in vivo kinase was endogenous PDK1 [16]. These results are in accord with our observation that active PDK1 *trans*-phosphorylates Ser-241 of λ PP-treated His₆-PDK1(Δ PH) (Fig. 1). In this case, His₆-PDK1(Δ PH) served as a 'kinase-defective' mutant in that it was unable to catalyze Ser-241 autophosphorylation. It is likely that endogenous PDK1 *trans*-phosphorylates Ser-241 of recombinant PDK1(Δ PH) constructs during expression in either Sf9 cells or in human cell lines employed for in vivo studies. Since PDK1(Δ PH) becomes immediately activated upon Ser-241 phosphorylation, further phosphorylation and activation of recombinant PDK1(Δ PH) can be exponentially propagated, yielding either the purified active enzyme (e.g., Sf9 cells) or the observed downstream catalytic effects (e.g., PKB phosphorylation in HEK 293 cells).

The observation that 5 μM λ PP-treated His₆-PDK1 sedimented as a monomeric species (Fig. 4) strongly suggests that the concentration independence and first-order progress curves observed for Ser-241 autophosphorylation occurs by an intramolecular or *cis* mechanism. The capability of PDK1-catalyzed Ser-241 *cis*-autophosphorylation is highlighted by X-ray structures, which have been determined for the catalytic domain of both wild type [21] and the S241A mutant of human PDK1 in complexes with ATP [33]. The overall structure of the inactive PDK1(S241A) mutant was surprisingly similar to the wild type PDK1 (root mean square deviation of 0.19 Å), showing little or no structural deviations in (i) the α B- and α C-helices, (ii) the PIF pocket of the N-lobe, and (iii) the bound ATP molecule. In addition, the PIF pocket of the S241A mutant retained its ability to bind with high affinity a peptide containing the *hydrophobic motif* of the PKC-related kinase-2 (HM-PRK2). The only striking deviation between the two structures was in positioning of the activation loop, where the C β carbon of Ala-241 was shifted by 10.1 Å compared with the C β carbon of phospho-Ser-241 in the wild type structure. The remarkable conformational plasticity of the activation loop of PDK1, together with the remaining conserved structural elements of the S241A and wild type pS241 catalytic domains, make catalysis of intramolecular transfer of the terminal phosphate of bound ATP to Ser-241 highly feasible.

Both in vitro kinetic studies, as well as in vivo studies using kinase-defective mutants, point towards an intramolecular mechanism for activation loop autophosphorylation of Tyr-216 in glycogen synthase kinase-3 (GSK3) [34] and Thr-575 in MEK kinase 1 (MEKK1) [35]. Similar to PDK1, in vitro kinetic studies indicated concentration-

independent first-order activation loop autophosphorylation of Tyr-416 in the Src tyrosine kinase [36,37], while in vivo studies showed that Tyr-416 of the kinase-defective mutant was *trans*-phosphorylated by another kinase [38]. Interestingly, a targeted molecular dynamics simulation generated a conformation of Src tyrosine kinase, whereby the phenolic oxygen of Tyr-416 arrived at the coordination sphere of one of the ATP-bound Mg^{2+} ions, placing it in position for attack of the γ -phosphate of ATP [39].

5. Conclusions

In summary, we have demonstrated that reconstitution of PDK1 catalytic activity occurs by sequential intramolecular Ser-241 and intermolecular Thr-513 autophosphorylation events (Fig. 3). Mutagenesis of Ser-241 showed that PDK1 catalytic activity absolutely required Ser-241 phosphorylation or a negatively charged side chain at this position, since the S241A mutant remained inactive. In this case, X-ray studies of the catalytic domain of PDK1 show that the negative charge is necessary to make specific activating contacts with residues from the C-terminal lobe and α C-helix [21]. However, the observation that both the T513A and T513E mutations were sufficient to maintain PDK1 catalytic activity (Fig. 5) suggests that a negative charge at residue 513 is not required for activation. Rather, these data suggest that chemical modification of residue 513 may cause dissociation of autoinhibitory contacts formed between the contiguous regulatory PH and catalytic kinase domains. Thus, there exists a possibility that compounds can be discovered or developed that will stabilize such autoinhibitory contacts [40,41].

Acknowledgments

This research was supported by a grant from the National Institute of General Medical Sciences (GM69868) to T.K.H. We kindly thank Dr. John S. Philo of Alliance Protein Laboratories (Thousand Oaks, CA) for sedimentation equilibrium data collection and analysis.

References

- [1] R.T. Peterson, S.L. Schreiber, *Curr. Biol.* 9 (1999) R521–R524.
- [2] D.R. Alessi, S.R. James, C.P. Downes, A.B. Holmes, P.R.J. Gaffney, C.B. Reese, P. Cohen, *Curr. Biol.* 7 (1997) 261–269.
- [3] D.R. Alessi, M. Deak, A. Casamayor, F.B. Caudwell, N. Morrice, D.G. Norman, P. Gaffney, C.B. Reese, C.N. MacDougall, D. Harbison, A. Ashworth, M. Bownes, *Curr. Biol.* 7 (1997) 776–789.
- [4] D. Stokoe, L.R. Stephens, T. Copeland, P.R. Gaffney, C.B. Reese, G.F. Painter, A.B. Holmes, F. McCormick, P.T. Hawkins, *Science* 277 (1997) 567–570.
- [5] L. Stephens, K. Anderson, D. Stokoe, H. Erdjument-Bromage, G.F. Painter, A.B. Holmes, P.R.J. Gaffney, C.B. Reese, F. McCormick, P. Tempst, J. Coadwell, P.T. Hawkins, *Science* 279 (1998) 710–714.
- [6] K.S. Walker, M. Deak, A. Paterson, K. Hudson, P. Cohen, D.R. Alessi, *Biochem. J.* 331 (1998) 299–308.
- [7] R.M. Biondi, A. Kieloch, R.A. Currie, M. Deak, D.R. Alessi, *EMBO J.* 20 (2001) 4380–4390.
- [8] B. Vanhaesebroeck, D.R. Alessi, *Biochem. J.* 346 (2000) 561–576.
- [9] A. Mora, D. Komander, D.M. van Aalten, D.R. Alessi, *Semin. Cell Dev. Biol.* 15 (2004) 161–170.
- [10] R.M. Biondi, *Trends Biochem. Sci.* 29 (2004) 136–142.
- [11] D. Komander, A. Fairservice, M. Deak, G.S. Kular, A.R. Prescott, C.P. Downes, S.T. Safrany, D.R. Alessi, D.M.F. van Aalten, *EMBO J.* 23 (2004) 3918–3928.
- [12] R.A. Currie, K.S. Walker, A. Gray, M. Deak, A. Casamayor, C.P. Downes, P. Cohen, D.R. Alessi, J. Lucocq, *Biochem. J.* 337 (1999) 575–583.

- [13] A. Casamayor, N.A. Morrice, D.R. Alessi, *Biochem. J.* 342 (1999) 287–292.
- [14] J. Park, M.M. Hill, D. Hess, D.P. Brazil, J. Hofsteenge, B.A. Hemmings, *J. Biol. Chem.* 276 (2001) 37459–37471.
- [15] M.J. Wick, K.R. Wick, H. Chen, H. He, L.Q. Dong, M.J. Quon, F. Liu, *J. Biol. Chem.* 277 (2002) 16632–16638.
- [16] M.J. Wick, F.J. Ramos, H. Chen, M.J. Quon, L.Q. Dong, F. Liu, *J. Biol. Chem.* 278 (2003) 42913–42919.
- [17] M.P. Scheid, M. Parsons, J.R. Woodgett, *Mol. Cell. Biol.* 25 (2005) 2347–2363.
- [18] N. Filippa, C.L. Sable, B.A. Hemmings, E. van Obberghen, *Mol. Cell. Biol.* 20 (2000) 5712–5721.
- [19] M.J. Wick, L.Q. Dong, R.A. Riojas, F.J. Ramos, F. Liu, *J. Biol. Chem.* 275 (2000) 40400–40406.
- [20] X. Gao, P. Yo, T.K. Harris, *Prot. Express. Purif.* 43 (2005) 44–56.
- [21] R.M. Biondi, D. Komander, C.C. Thomas, J.M. Lizcano, M. Deak, D.R. Alessi, D.M.F. van Aalten, *EMBO J.* 21 (2002) 4219–4228.
- [22] T.M. Laue, B.D. Shah, T.M. Ridgeway, S.L. Pelletier, in: S.E. Harding, A.J. Rowe, J.C. Horton (Eds.), *Analytical Ultracentrifugation in Biochemistry and Polymer Science*, Royal Society of Chemistry, Cambridge, 1992, pp. 90–125.
- [23] J.S. Philo, J. Talvenheimo, J. Wen, R. Rosenfeld, A.A. Welcher, T. Arakawa, *J. Biol. Chem.* 269 (1994) 27840–27846.
- [24] J.S. Philo, *Methods Enzymol.* 321 (2000) 100–120.
- [25] R.M. Biondi, P.C.F. Cheung, A. Casamayor, M. Deak, R.A. Currie, D.R. Alessi, *EMBO J.* 19 (2000) 979–988.
- [26] C.T. Zimmerle, C. Frieden, *Biochem. J.* 258 (1989) 381–387.
- [27] W.A. Lim, *Curr. Opin. Struct. Biol.* 12 (2002) 61–68.
- [28] K.E. Prehoda, W.A. Lim, *Curr. Opin. Cell Biol.* 14 (2002) 149–154.
- [29] D. Kern, E.R.P. Zuiderweg, *Curr. Opin. Struct. Biol.* 13 (2003) 748–757.
- [30] M. Buck, W. Xu, M.K. Rosen, *J. Mol. Biol.* 338 (2004) 271–285.
- [31] D.W. Leung, M.K. Rosen, *Proc. Natl. Acad. Sci. USA* 102 (2005) 5685–5690.
- [32] T. Gao, F. Furnari, A.C. Newton, *Mol. Cell* 18 (2005) 13–24.
- [33] D. Komander, G. Kular, M. Deak, D.R. Alessi, D.M.F. van Aalten, *J. Biol. Chem.* 280 (2005) 18797–18802.
- [34] A. Cole, S. Frame, P. Cohen, *Biochem. J.* 377 (2004) 249–255.
- [35] J.C. Deak, D.J. Templeton, *Biochem. J.* 322 (1997) 185–192.
- [36] Y. Sugimoto, E. Erikson, Y. Graziani, R.L. Erikson, *J. Biol. Chem.* 260 (1985) 13838–13843.
- [37] H. Piwnicka-Worms, K.B. Saunders, T.M. Roberts, A.E. Smith, S.H. Cheng, *Cell* 49 (1987) 75–82.
- [38] J.A. Cooper, A. MacAuley, *Proc. Natl. Acad. Sci. USA* 85 (1988) 4232–4236.
- [39] J. Mendieta, F. Gago, *J. Mol. Graph. Model.* 23 (2004) 189–198.
- [40] T.K. Harris, *IUBMB Life* 55 (2003) 117–126.
- [41] T.K. Harris, *Methods Mol. Biol.* 316 (2005) 199–225.